DEGENERATE FOUR-WAVE MIXING IN SEMICONDUCTORS AND FERROELECTRICS

M. Klein, R. Jain, G. Valley

JOURNAL DE PHYSIQUE
Colloque C2, supplément au n°3, Tome 44, mars 1983 *page* C2-149

DEGENERATE FOUR-WAVE MIXING IN SEMICONDUCTORS AND FERROELECTRICS

M.B. Klein, R.K. Jain and G.C. Valley

Hughes Research Laboratories, 3011 Malibu Canyon Road, Malibu, CA 90265, U.S.A.

Résumé - Les semiconducteurs et les ferroélectriques sont des candidats prometteurs pour des applications variées du mélange de quatre ondes dégénérées. Dans ce propos, nous allons passer en revue les mécanismes non linéaires dans chaque matériau et comparer les performances de chaque type pour les applications au mélange de quatre ondes dégénérées.

Abstract - Semiconductors and ferroelectrics are promising candidate materials for a variety of applications of degenerate four-wave mixing. In this talk, we will review nonlinear mechanisms in each material and compare the performance of both types of materials for degenerate four-wave mixing applications.

I. INTRODUCTION

In recent years, the technique of degenerate four-wave mixing (DFWM) has been used in a variety of applications, including phase conjugation, aberration correction, image processing, spectral filtering, phase conjugate resonators, etc. Two classes of nonlinear materials which show great promise for DFWM applications are semiconductors and ferroelectrics. In semiconductors, large nonlinearities can be obtained via a variety of optical transitions, most notably the interband excitation of a free carrier plasma. The associated response times are relatively fast (10^{-9}-10^{-6}sec), and are determined by the buildup and decay of carrier populations. In the case of ferroelectrics, the space charge electric fields generated by carrier generation, migration and subsequent trapping, combined with large values of electro-optic coefficients lead to large nonlinearities via the photorefractive effect. The response time for this effect is dependent upon the incident intensity, with measured values ranging from 10^{-9}-10^{-8}sec for pulsed laser excitation to 10^{-3}-10^{-1}sec for CW excitation. In this paper, we will briefly review some of the principal nonlinear mechanisms in both semiconductors and ferroelectrics, present DFWM results for typical materials, and compare the performance of both types of materials for DFWM applications.

The principal configuration of interest is the backward DFWM configuration, in which three waves at frequency ω are incident on the nonlinear medium. Two of the waves are strong counterpropagating pumps travelling in the forward and backward directions with amplitudes $\vec{E}_f$ and $\vec{E}_b$, respectively. The third input wave is a weak probe (amplitude $\vec{E}_p$) which makes a small angle θ with respect to the pump wave. Phase matching then requires that the phase conjugate signal wave (amplitude $\vec{E}_c$) be radiated in a direction backward to the probe wave. The nonlinear or DFWM reflectivity is defined as

$$R = \frac{|\vec{E}_c|^2}{|\vec{E}_p|^2} \quad . \tag{1}$$

For the backward DFWM configuration there are typically two separate grating contributions to the reflectivity R, as shown in Figure 1. In many cases one grating term is dominant over the other, but this must be verified for each experiment. For example, in semiconductors in which the nonlinearity is due to the

optical generation of free carriers, the contribution from the small period grating is usually negligible, due to washout by diffusion. By contrast, the diffusion contribution to the photorefractive nonlinearity in ferroelectrics favors the small period grating. The spatial frequency response of semiconductors and ferroelectrics will be compared in more detail in Section IV.

Finally, we note that in semiconductors there are other contributions to the nonlinear polarization beside the two gratings discussed above. The added terms are generally smaller and include contributions from two-photon (and higher order) absorption and self diffraction, and do not necessarily require the establishment of a spatial grating. For a more detailed review of mechanisms and materials for DFWM in semiconductors, see Reference [1].

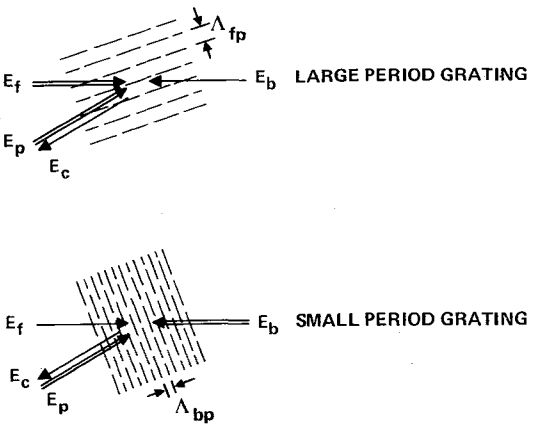

Figure 1: Grating contributions to the nonlinear reflectivity. The large period grating is created by the interference of $\vec{E}_f$ and $\vec{E}_p$, and is read out by $\vec{E}_b$. The small period grating is created by the interference of $\vec{E}_b$ and $\vec{E}_p$, and is read out be $\vec{E}_f$.

II. DFWM IN SEMICONDUCTORS

Semiconductors are unique in that they possess an unusually large variety of nonlinear optical mechanisms that can be used for DFWM. This abundance of nonlinear mechanisms is largely due to the presence of free carrier states (in addition to the bound electron states that are present in all optical materials), and to the ease with which free carriers can be optically generated. Other discrete states due to impurities and excitons can also contribute to the nonlinear behavior. In our discussion of DFWM in semiconductors, we first present some general observations on the nonlinear polarization density in these materials, and then describe specific mechanisms and experiments.

In a medium with a local response such as a semiconductor, the nonlinear polarization density loading to the DFWM signal can be written as a sum of 3rd and higher odd order nonlinear terms in the applied electric fields. The order of the susceptibilities and the specific terms which contribute significantly to the DFWM signal depend on the specifics of the nonlinear interaction. For instance, in the case where the nonlinear mechanism is due to two-photon transitions from the valence band to the conduction band, terms involving both third order and fifth order nonlinear susceptibilities will generally be significant, and the dominance of one over the other will depend on the specific experimental conditions. By the same token, all higher order terms become important when significant population changes are caused by the radiation, such as near the saturation intensity of a resonant transition. We note however, that the third order terms are dominant for the most important nonlinearities at low intensities.

The various electronic nonlinearities in semiconductors can be divided into non-resonant and resonant categories. The first two nonlinearities described below -- namely, anharmonic motion of bound electrons and nonlinear motion of free carriers--are by and large nonresonant, and are generally characterized by very fast speeds, but relatively small nonlinear susceptibilities. Most of the remaining nonlinearities described are resonant, i.e., involve redistribution of populations, and are consequently limited by speeds corresponding to energy buildup and relaxation times. Nevertheless, a major advantage of the resonant nonlinearities is the large enhancements in the values of $\chi^{(3)}$ that may be possible, e.g. from $\sim 10^{-11}$ esu for the bound electron nonlinearity in Ge to $\sim 10^{-1}$ esu for interband transitions in InSb and HgCdTe.

One of the first electronic nonlinearities studied in semiconductors [2], and the one most commonly used in early (nondegenerate) four-wave mixing experiments is due to the anharmonic motion of bound electrons far from their resonant frequencies. This nonlinearity is present in all crystalline solids, and is the dominant nonlinearity in intrinsic semiconductors at frequencies well below the bandgap. Furthermore, this nonlinearity was the first one for which experimental results on DFWM and phase conjugation in a semiconductor were reported [3]. Using a third-order susceptibility of $\sim 2.5 \times 10^{-11}$ esu in Ge at 10.6 μm, reflection returns of ~2% were reported at pump intensities of ~40 MW/cm^2.

In doped semiconductors with moderately large free carrier concentrations ($\gtrsim 10^{15}$/cm^3), significant nonlinearities may be present due to the nonlinear motion and energy relaxation of free carriers in response to the driving optical fields [4,5]. Such nonlinearities can be particularly large in narrow gap semiconductors (such as InSb, InAs and HgCdTe), because of the large nonparabolicity of the conduction bands. Early studies of this nonlinearity [6] used four-wave mixing with nondegenerate frequencies. Recently Yuen and Wolff [5] have clarified the important role of carrier energy relaxation with experiments on nondegenerate four-wave mixing, and have demonstrated a significant enhancement in the nonlinear susceptibility as the degenerate frequency case is approached. The Yuen and Wolff model for these free carrier nonlinearities leads to an estimated susceptibility for DFWM in InSb (at 10.6 μm) of $\sim 10^{-7}$ esu. Nevertheless, no four-wave mixing experiments with degenerate frequencies have been reported in which the nonlinear behaviour is unambiguously attributed to the nonlinear motion of free carriers.

Several effects associated with transitions in semiconductors can lead to large nonlinearities for DFWM. These include free carrier plasma generation via valence-to-conduction band transitions, saturation of interband absorption, and saturation of exciton absorption. The largest nonlinearities have been obtained via optically induced free carrier generation. These nonlinearities were first studied by Woerdman [7] in 1971, and more recently by Jain, et. al. [8-11].

The nonlinear polarization density for the backward DFWM configuration can then be written as

$$P^{NL} = \chi_{fp}^{(3)} (\vec{E}_f \cdot \vec{E}_p^*) \vec{E}_b + \chi_{bp}^{(3)} (\vec{E}_b \cdot \vec{E}_p^*) \vec{E}_f \quad . \tag{2}$$

The susceptibility $\chi_{ip}^{(3)}$ corresponds to the grating term (see Figure 1) obtained from the interference of the probe wave with pump beam i (with i ≡ f or b). Since the plasma nonlinearity is strongly affected by carrier diffusion, the susceptibilities $\chi_{ip}^{(3)}$ are expected to be functions of the grating spacing Λ, and thus strong functions of the angle θ between the forward and probe waves (especially near θ=0).

In their analysis, Jain and Klein [8] derived expressions for $\chi^{(3)}$ in two limits, depending on the relative values of the pulse length τ_L and the effective carrier delay time τ given by

$$(\tau)^{-1} = (\tau_R)^{-1} + (\tau_D)^{-1} \quad , \tag{3}$$

where τ_R is the recombination time and τ_D is the ambipolar diffusional delay time given by

$$\tau_D = \Lambda^2 / 4\pi^2 D_a \quad , \tag{4}$$

where D_a is the ambipolar diffusion coefficient.

For long pulses or cw operation ($\tau_L > \tau$) the nonlinear susceptibility is given by

$$\chi^{(3)} = -\frac{\eta\alpha\, nce^2\tau}{8\pi\, m^*_{eh}\, \hbar\omega^3}\left[\frac{\omega_g^2}{\omega_g^2-\omega^2}\right] \tag{5}$$

where η is the quantum efficiency for generation of an electron-hole carrier pair, α is the absorption coefficient for carrier pair generation, m^*_{eh} is the reduced optical mass of the electron-hole pair, and ω_g is the photon frequency corresponding to the direct band edge. For short pulses ($\tau_L < \tau$) the nonlinear susceptibility is given by

$$\chi^{(3)} = -\frac{\eta\alpha\, nce^2\tau_L}{16\pi\, m^*_{eh}\, \hbar\omega^3}\left[\frac{\omega_g^2}{\omega_g^2-\omega^2}\right] \tag{6}$$

The term in brackets in Eqs. (5) and (6) is due to interband transitions and leads to a large enhancement in $\chi^{(3)}$ near the direct band edge. The ω^{-3} factor in these expressions suggests that particularly large values of $\chi^{(3)}$ can be obtained at long wavelengths. Finally, the occurrence of τ in Eq. (5) is a direct consequence of the limited speed of the plasma nonlinearity, which is dependent on both the recombination and diffusion times of the carriers.

In the experiments of Jain and Klein [8,9] the peak power reflectivity in Si at 1.06 μm was measured using a Nd:YAG laser with a 15 ns pulse width; typical experimental data are plotted in Figure 2. For low pump intensities the reflectivity varied quadratically with the pump intensity, as expected for a third order interaction. From such data, an experimental susceptibility $\chi^{(3)} = 1.1\times10^{-7}$ esu was obtained. This compares well with the calculated value $\chi^{(3)} = 8\times10^{-8}$ esu for the large period grating. The calculated contribution from the small-period grating is smaller by a factor of $\sim10^4$. For a given pump intensity, the largest signal was observed for a 1.0 mm sample thickness, which is consistent with optimum interaction of the counterpropagating pump beams in our samples with $\alpha = 10\ cm^{-1}$. At high pump intensities, the signals begin to saturate, due to free carrier absorption. Note the large reflection return (180%) for the 0.5 mm sample at ~10 MW/cm^2.

In a given semiconductor, the optical frequencies for which the plasma nonlinearity is optimized are limited to a small range near the bandgap. At lower frequencies, little carrier generation occurs, and at higher frequencies the sample absorption is too large. For DFWM applications requiring use of a given laser wavelengths, it is very useful to select a semiconductor with a bandgap "tuned" to resonance with the laser frequency. One means for achieving this is to use ternary alloys with variable composition. One convenient mixed semiconductor system that spans a broad range in the visible spectral region is the CdS_xSe_{1-x} system. This compound may be doped in an amorphous glass matrix, and samples of such material can be obtained conveniently and inexpensively in the form of shart cut-off color glass filters. Each CdS_xSe_{1-x}-doped glass contains isolated microcrystals (typically 100Å-1000Å in size) of fixed composition x suspended in a glass matrix. The individual microcrystals are of uniform composition throughout the sample and oriented randomly. The bulk material is thus isotropic and insulating.

DFWM due to plasma generation in the CdS_xSe_{1-x} glasses has been studied by Lind and Jain [12], using a variety of pulsed ($\lesssim$15 ns) laser sources with wavelengths in the range 0.532 - 0.694 μm. Susceptibilities of the order of 10^{-8} esu and reflectivities of up to 10% (at pump powers of ~1 MW/cm^2) were measured.

One interesting consequence of the microscopic structure of the CdS_xSe_{1-x}-doped glasses is that the DFWM signal due to the small-period grating was found to be comparable to the signal due to the large-period grating. This is due to the fact that the semiconductor crystallites are generally much smaller (100Å-1000Å) than even the 1030Å period of the small-period grating. Thus, unlike the situation in bulk semiconductors, the free carrier plasma is effectively confined to these isolated pockets, and plasma diffusion does not reduce the diffraction efficiency of the

small-period grating. To our knowledge, this is the only "diffusion-free" DFWM or transient grating experiment reported.

The longest wavelengths at which DFWM experiments have been performed are the 10 μm CO_2 laser wavelengths. A particularly useful nonlinear material for this spectral region is the alloy $Hg_{1-x}Cd_xTe$, whose bandgap can be tuned throughout the range of CO_2 laser lines by adjustment of the composition. The usefulness of the plasma nonlinearity in HgCdTe for DFWM at long wavelengths was first predicted by Jain and Klein [8], and DFWM measurements on room temperature samples with pulsed CO_2 laser radiation were carried out by Jain and Steel [10]. Using 180 ns pulses from a CO_2 TEA laser and an x=0.2 n-type sample ($\hbar\omega_q$ = 0.16 eV), a third-order susceptibility of 5.4×10^{-6} esu was measured, and good agreement was obtained with the value calculated using the plasma model.

One important conclusion made by Jain and Steel [10] was that the size of the nonlinearity in the room temperature HgCdTe samples was limited by the short carrier recombination time (due to Auger recombination) and the mismatch between the photon energy and the bandgap. The predicted that with the use of lower temperatures, and samples with an appropriate match of the low temperature bandgap to the laser photon energy, third order susceptibilities greater than 10^{-2} esu would be possible. In subsequent work [11], such large susceptibilities were in fact demonstrated, consistent with the above predictions. Using an unfocused 1 W cw CO_2 (P(20) transition at 10.6 μm) and an x=0.22 n-type sample, a strong increase in the DFWM signal was observed as the sample temperature was lowered, with a maximum signal observed for $T \approx -145°C$. The reduction in the DFWM signal for lower temperatures is due to the rapid increase in the absorption coefficient resulting from the enhanced bandgap resonance. At the optimum temperature a reflectivity of ~2.2% was observed at a mean pump intensity of only 10 W/cm^2 (see Figure 3), implying a third order susceptibility of over 5×10^{-2} esu. Similar values of $\chi^{(3)}$ have also ben observed in HgCdTe by Khan et. al. [13]. Note that the reported values of $\chi^{(3)}$ are larger than those measured by Miller, et. al. [14] in a comparable DFWM experiment in InSb at 5.3 μm.

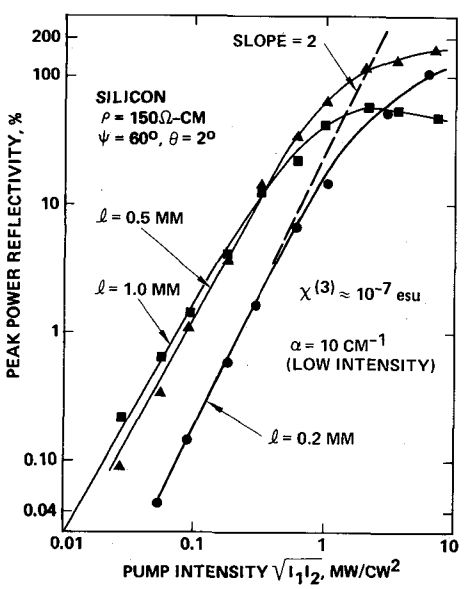

Figure 2: Peak power reflectivity vs. pump intensity for DFWM in silicon at 1.06 μm. Results for three values of sample thickness are shown.

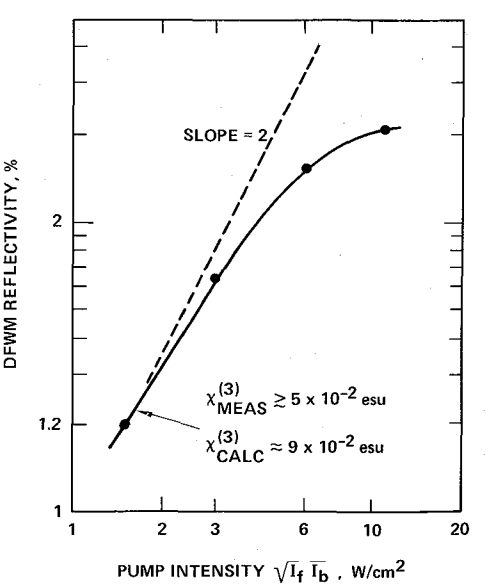

Figure 3: DFWM reflectivity vs pump intensity for $Hg_{0.78}Cd_{0.22}Te$ at 10.6 μm, with $T \approx -145°C$.

In summary, semiconductors are promising materials for DFWM over a range of wavelengths extending from the visible to the middle IR. The nonlinearity due to interband plasma generation is particularly large, especially at long wavelengths. One constraint imposed by such a nonlinearity is that the laser photon energy must be in near resonance with the bandgap of the material of interest. Mixed-composition semiconductors with tunable bandgap energies aid significantly in establishing such an energy coincidence. Finally, the dependence of the plasma nonlinearity on the buildup and decay of free carriers influences both the speed and the spatial frequency response of the nonlinearity. This will be discussed later in relation to the analogous characteristics for ferroelectrics.

III. GRATING FORMATION AND DFWM IN FERROELECTRICS

Some of the most attractive materials for practical applications of DFWM via the photorefractive effect are ferroelectric materials such as $LiNbO_3$, $BaTiO_3$, SBN and $KNbO_3$, and nonpolar electro-optic materials such as BSO and BGO. Ferroelectric materials are particularly promising because their large electro-optic coefficients lead to large grating efficiencies and DFWM reflectivities, in spite of their relatively slow speeds. For example, DFWM reflectivities exceeding 2000% have been reported in $BaTiO_3$ [15] using a cw laser at a power level of ~5 mW. This large reflectivity was obtained by orienting the crystal to exploit the large electro-optic coefficient $r_{42} = 840 \times 10^{-12}$ m/V. One important characteristic of grating formation in photorefractive materials is that for certain experimental conditions the refractive index grating may be shifted in space relative to the intensity grating formed by the interfering light beams. This shifted grating, which is nearly unique to photorefractive materials (in the steady state), allows the construction of novel devices such as image amplifiers [16] and phase conjugate resonators [15,17,27].

Two separate models for calculating the grating space charge fields and response times have been formulated: the hopping model [18] assumes that carrier transport occurs via hopping from a filled donor site to a neighboring empty trap. This model was originally developed to describe electrical conduction in semi-insulating materials and amorphous semiconductors. The band transport model (developed most completely by Kukhtarev and co-workers [19,20]) assumes that electrons (or holes) are excited from filled donor (or acceptor) sites to the conduction (or valence) band, where they migrate to dark regions in the crystal by drift, diffusion or the bulk photovoltaic effect before recombining into an empty trap. The band transport model has been developed to a greater degree and is in wider use in the literature; however, both models invoke the physical separation of charge, and are thus nonlocal in nature. As a result, the nonlinear behavior of photorefractive materials cannot be characterized by a nonlinear polarization, or by conventional nonlinear susceptibilities.

In order to analyze DFWM properties of ferroelectrics, we first require expressions for the amplitude and spatial phase of the space charge electric field. The required expressions have been derived (using the band transport model) for specific limiting cases. One case of relevance for many experiments is $m \ll 1$, where m is the fractional modulation of the input irradiance. For this case [19,20] the solution for the steady state space charge field amplitude is

$$E_{sc} = m\, E_q \left[\frac{(E_o^2 + E_D^2)}{E_o^2 + (E_D + E_q)^2} \right]^{1/2} \tag{7}$$

where

E_o = Applied drift field (normal to grating planes),

$E_D = \frac{kT}{e} k_g$ (diffusion field),

and

$E_q = \frac{4\pi e N_A}{\varepsilon k_g}$ (limiting space charge field).

In the above expressions, k is the Boltzman constant, k_g is the grating wave number, N_A is the density of empty traps, and ε is the dielectric constant. The field E_q is that which results from the separation of all available charges by one grating period. The spatial phase ψ of E_{sc} (relative to the irradiance) is given by

$$\tan \psi = \frac{E_D}{E_o} \left[1 + \frac{E_D}{E_o} + \frac{E_o^2}{E_D E_q} \right] . \tag{8}$$

In general, $E_D \ll E_q$ so that with no applied drift field $E_{sc} \approx m\, E_D$, and $\psi = \frac{\pi}{2}$. This is the diffusion limit, for which a characteristic spatial phase shift between the irradiance and the space charge field is observed. As the applied drift field is increased from zero, we have $E_{sc} \approx m\, (E_o^2+E_D^2)^{1/2}$, and the spatial phase is intermediate between 0 and $\frac{\pi}{2}$. Finally, for large values of drift field ($E_o > E_q$), the space charge field saturates at $E_{sc} \approx m\, E_q$, and the phase shift ψ is one again $\pi/2$.

Note that for small values of the drift field ($E_o < E_q$), the space charge field is independent of all material parameters. In this case the induced refractive index variation is determined entirely by the relevant electro-optic coefficient. Thus for large values of index modulation, materials with large values of electro-optic coefficient are desirable. However, materials in this category (e.g. $BaTiO_3$, SBN) tend to be slow. Specifically, the band transport solutions for small modulation fraction give the write or erase time [20] as

$$\tau_e = \tau_w \approx \tau_{di} \tag{9}$$

where τ_{di} is the dielectric relaxation time,

$$\tau_{di} = \frac{\varepsilon}{4\pi\sigma} = \frac{\varepsilon}{4\pi n e \mu} , \tag{10}$$

where σ is the conductivity, n is the free carrier density, and μ is the mobility. If the conductivity is dominated by the contribution from photocarriers, then a simple rate equation solution gives

$$n = \frac{s I_o}{\gamma_R} \frac{N_D - N_A}{N_A} , \tag{11}$$

where s is the photoionization cross section, γ_R is the recombination rate coefficient, $N_D - N_A$ is the density of filled traps, N_A (as defined earlier) is the density of empty traps, and I_o is the average irradiance. By combining Eqs. (10) and (11), we obtain

$$\tau_{di} = \left(\frac{\varepsilon\, \gamma_R}{4\pi e \mu s} \right) \frac{1}{I_o} \frac{1}{R} , \tag{12}$$

where the reduction ratio R is defined as

$$R = \frac{N_D - N_A}{N_A} . \tag{13}$$

The quantity in parentheses in Eq. (12) can be considered as a material figure of merit, having units of energy/unit area. Once a material is chosen, only limited experimental control over this quantity is possible. However, the quantity R can be varied over many orders of magnitude by reduction or oxidation of a given sample. It is clear from Eq. (12) that increasing R through chemical reduction can

significantly reduce τ_{di}. Values of R as high as 10 are not hard to achieve in many cases, and in some materials (e.g. BSO) values of R on the order of 10^3 are typical [21]. Note also the I_0^{-1} dependence in Eq. (12), indicating the direct relation between speed and irradiance.

In our review of grating formation in photorefractive materials, it was assumed that the incident fields in each volume element are known. In an actual DFWM experiment, only the input fields (e.g. $\tilde{E}_f$, $\tilde{E}_b$ and $\tilde{E}_p$) are known. The complete grating solution requires the substitution of the refractive index change (as a function of the local fields) into the wave equations which describe the propagation through the material. This results in four coupled wave equations, compared with two for the simpler case of two-wave mixing. In these equations, the contribution from both the small-period and large-period gratings must be considered, as well as self interaction effects. Several approaches to the solution of the coupled wave equations have been presented [22-24], and in certain cases, bistability and hysteresis have been predicted [25].

IV. COMPARISONS BETWEEN SEMICONDUCTORS AND FERROELECTRICS

The nonlinear mechanisms in semiconductors are quite different from the photorefractive nonlinearity, leading to many differences in behavior between the two materials for DFWM applications. Two specific comparisons are discussed below; to make our discussion more specific, we will assume that the dominant semiconductor nonlinearity is that due to interband plasma generation.

A. RESPONSE TIME

In semiconductors the response time is determined by recombination and diffusion (see Eq. 3). For example, in the experiments of Jain and Klein [8] in silicon ($\tau_R \approx 10^{-6}$ sec) the decay times of both gratings were dominated by diffusion, and were calculated to be τ_{fp} = 61 nsec and τ_{bp} = 0.4 psec. Since the nonlinear susceptibility for each grating is proportional to the grating decay time, the relatively fast decay times in silicon are accompanied by reduced susceptibilities compared with those which could be obtained with longer pulses and larger grating spacings.

The response time in ferroelectric materials for cw experiments can be approximated in many cases by the dielectric relaxation time (Eqs. 12 and 14) [20]. As mentioned earlier, faster response times can be obtained by reducing the sample and by increasing the irradiance.

B. SPATIAL FREQUENCY DEPENDENCE

The spatial frequency dependence of the nonlinear susceptibility in semiconductors is very different from that of the grating efficiency in photorefractive materials, due to the differing effects of diffusion in both materials, and the influence of an applied drift field in photorefractive materials. In semiconductors, diffusion reduces the grating response at high spatial frequencies, as may be seen by combining Eqs. 2-5:

$$\chi^{(3)} = A\tau = A \frac{(\Lambda^2/4\pi^2 D_a)\tau_R}{(\Lambda^2/4\pi^2 D_a) + \tau_R} \qquad (14)$$

where A is a constant. Eq. (14) is plotted in Figure 4 for silicon at 1.06 μm (D_a = 15 cm^2/sec, $\tau_R = 10^{-6}$ sec). Note the rapid decrease in $\chi^{(3)}$ for spatial frequencies on the order of 4 cycles/mm (250 μm grating period). In the pulsed experiments of Jain and Klein [8] the larger grating period was 60 μm, leading to a value of $\chi^{(3)}$ approx. 10 times lower than optimum.

In photorefractive materials the grating efficiency η is given by

$$\eta \sim (\Delta n)^2 \sim E_{sc}^2 \quad (n<<1) \quad . \qquad (15)$$

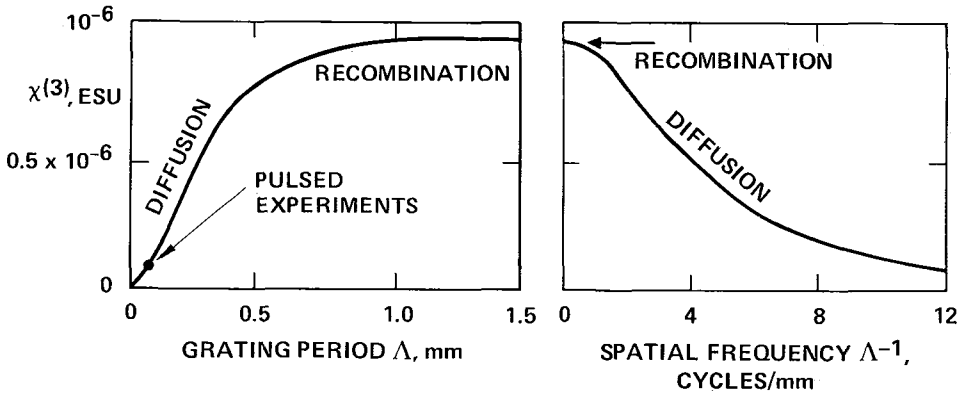

Figure 4: Variation of $\chi^{(3)}$ with grating period and spatial frequency for Si at 1.06 μm.

By combining with Eq. (7) and the definitions for E_D and E_q, the spatial frequency dependence can be determined. Results obtained by Huignard [26] for BSO are plotted in Figure 5. For E_0=0, diffusion favors small grating periods, until the limit E_D=E_q is reached. The application of a drift field can compensate for the spatial frequency imposed by diffusion, leading to a flat response when E = 2 KV/cm. In this case the limiting spatial frequency (for which rolloff in η becomes significant) is nearly 3 orders of magnitude larger than the analogous value in silicon.

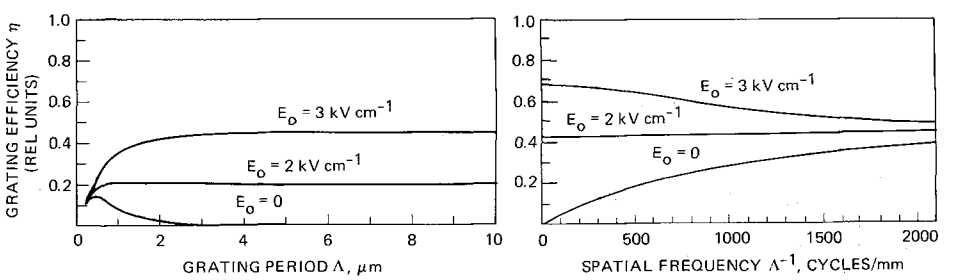

Figure 5: Variation of grating efficiency with grating period and spatial frequency for BSO (after Reference [26]).

V. CONCLUSIONS

Semiconductors and ferroelectrics both have large nonlinearities for DFWM applications. However, the different origin of the nonlinear effects leads to many different properties. For example, the plasma nonlinearity in semiconductors is exceptionally large in the infrared (using small bandgap materials), while photorefractive materials are most sensitive in the visible, and have little or no response in the infrared. At their preferred wavelengths, both materials can be used to generate large DFWM returns with cw lasers. The nonlocal nature of the photorefractive nonlinearity leads to several unique characteristics such as spatially shifted refractive index gratings, slower speeds for cw experiments, and long lifetimes for holographic storage. In many DFWM applications, large values of nonlinear reflectivity are required at low cw power levels. Photorefractive

materials with large electro-optic coefficients (such as $BaTiO_3$ and SBN) appear promising for these applications. Existing samples of these materials are relatively slow, but it is hoped that improved materials processing can increase speed while maintaining efficiency.

REFERENCES

1. R.K. Jain and M.B. Klein, "Degenerate Four-Wave Mixing in Semiconductors," in Optical Phase Conjugation, R.A. Fisher, Ed. (Academic Press, New York, 1983).
2. J.J. Wynne and G.O. Boyd, Appl. Phys. Lett. 12, 191 (1968).
3. E.E. Bergmann, I.J. Bigio, B.J. Feldman and R.A. Fisher, Opt. Lett. 3, 82 (1978).
4. P.A. Wolff and G.A. Pearson, Phys. Rev. Lett. 17, 1015 (1966).
5. S.Y. Yuen and P.A. Wolff, Appl. Phys. Lett. 40, 457 (1982).
6. C.K.N. Patel, R.E. Slusher and P.A. Fleury, Phys. Rev. Lett. 17, 1011 (1966).
7. J.P. Woerdman, Opt. Comm. 2, 212 (1971).
8. R.K. Jain and M.B. Klein, Appl. Phys. Lett. 35, 454 (1979).
9. R.K. Jain, M.B. Klein and R.C. Lind, Opt. Lett. 4, 328 (1979).
10. R.K. Jain and D.G. Steel, Appl. Phys. Lett. 37, 1 (1980).
11. R.K. Jain and D.G. Steel, Conf. on Laser Eng. and Electro-Optics, Paper FL3, Washington, D.C. (1981); ____, Opt. Comm. 43, 72 (1982).
12. R.K. Jain and R.C. Lind, XI Int. Quantum Electron. Conf., Boston, Mass. (1980), Paper E.4.
13. M.A.Khan, R.L.H. Bennett, and P.W. Kruse, Opt. Lett. 6, 560 (1981).
14. D.A.B. Miller, R.G. Harrison, A.M. Johnston, C.T. Seaton and S.D. Smith, Opt. Comm. 32, 478 (1980).
15. J. Feinberg, and R.W. Hellwarth, Opt. Lett. 5, 519 (1980).
16. V. Markov, S. Odulov and M. Soskin, Opt. Laser Tech. 5, 95 (1979).
17. J.O. White, M. Cronin-Golomb, B. Fischer and A. Yariv, Appl. Phys. Lett. 40, 450 (1982).
18. J. Feinberg, D. Heiman, A.R. Tanguay, Jr. and R.W. Hellwarth, J. Appl. Phys. 51, 1297 (1980).
19. N.V. Kukhtarev, V.B. Markov, S.G. Odulov, M.S. Soskin and V.L. Vinetskii, Ferroelectrics 22, 949 (1979).
20. N.V. Kukhtarev, Sov. Tech. Phys. Lett. 2, 438 (1976).
21. M. Peltier and F. Micheron, J. Appl. Phys. 48, 3683 (1977).
22. B. Fischer, M. Cronin-Golomb, J.O. White and A. Yariv, Opt. Lett. 6, 519 (1981).
23. M. Cronin-Golomb, J.O. White, B. Fischer and A. Yariv, Opt. Lett. 7, 313 (1982).
24. N.V. Kukhtarev and S.G. Odoulov, Proc. SPIE Conf. on Optics and Photonics Applied to Communication and Processing, 213, 2 (1979).
25. N.V. Kukhtarev and T.I. Semenets, Sov. Phys. Tech. Phys. 26, 1159 (1982).
26. J.P. Huignard, J.P. Herriau, G. Rivet and P. Gunter, Opt. Lett. 5, 102 (1980).
27. R.K. Jain and G.J. Dunning, Opt. Lett. 7, 420 (1982).